Jaynes-Cummings model under continuous measurement: Weak chaos in a quantum system induced by unitarity collapse

Tsuyoshi Fukuo
Department of Applied Physics, Osaka City University, Sumiyoshi-ku, Osaka 558-0022, Japan

Tetsuo Ogawa*
Department of Physics, Tohoku University, Aoba-ku, Sendai 980-8578, Japan

Katsuhiro Nakamura
Department of Applied Physics, Osaka City University, Sumiyoshi-ku, Osaka 558-0022, Japan
(Received 24 March 1998)

We show that a system managed by quantum theory bears chaotic behavior induced by *unitarity collapse* in its time development. Nonunitary time evolution of the Jaynes-Cummings (JC) model, the interacting system consisting of two subsystems (a two-level atom and a quantized photon field), under a continuous quantum-nondemolition (QND) measurement of the photon number is investigated. In the regime of weak coupling between the subsystems, the measured system shows the Rabi oscillation and the decrease of the photon number variance, which mimic the unmeasured JC system and the photon field under the continuous QND photodetection, respectively. In the strong-coupling regime, the quantum system shows a nonintegrable nature, that is, it yields *weak chaos* characterized by both the broad continuous power spectrum and the decaying correlation function due to the lack of quantum recurrence. [S1050-2947(98)03910-9]

PACS number(s): 42.50.Ct, 03.65.Bz, 05.45.+b, 42.50.Dv

I. INTRODUCTION

Despite the accumulation of considerable works on quantum theory of chaotic systems, there exists a prevailing belief that, due to the linearity of the Schrödinger equation, the quantum system exhibits no chaos characterized by standard diagnostics of the positive Lyapunov exponent. Even if its classical counterpart would show chaos, the Schrödinger equation describes only a time-periodic or quasiperiodic wave and inevitably excludes any solution representing temporal chaos or turbulence in general [1].

Such a belief, however, could be valid only if the quantum system is assumed to be ''closed,'' that is, to be confined in an infinite-Q cavity without leakage and not to interact with the other subsystems. In practical experiments, signals out of the system should be measured by using proper apparatus and the measurement process is usually continued for a long duration, referred to as the continuous measurement. The continuous measurement action enforces the system to couple with the large degrees of freedom outside, and ''readout'' of the measurement information will give a continuous back action on the measured system. The process of this kind does disturb the quantum system via continuous reduction of wave packets, which cannot be described by the time-dependent Schrödinger equation. Therefore, the time evolution induced by the continuous measurement is intrinsically time-irreversible and nonunitary.

Then, what should take place if the classically nonintegrable quantum system has been continuously measured? Under such a circumstance, temporal evolution of the system is governed not only by the Schrödinger equation but also by the continuous state reduction caused by the measurement back action. So there will appear a possibility that a quantum system shows temporal chaos due to the lack of quantum recurrence. The subject has a similarity to that on decoherence induced when the quantum system is coupled with the environment [2]. The decoherence phenomenon implies the environment-induced suppression of quantum suppression of chaos, thereby eventually recovering the chaos in quantum dynamics. Despite the similarity between the environment-induced decoherence and continuous measurement, the latter is governed by von Neumann's peculiar nonunitary process. Therefore, the continuous measurement of a classically chaotic quantum system has its own right to be investigated as a perfectly independent theme.

In this paper, we investigate the temporal evolution of the quantum system under the continuous measurement, and demonstrate within quantum theory that the system shows *weak chaos* induced by the unitarity collapse in the course of its time development [3]. Concretely, we employ as such a system the Jaynes-Cummings model, which consists of a two-level atom interacting with a single-mode quantized photon field, and consider the continuous quantum nondemolition (QND) photon counting as a continuous measurement strategy (see Fig. 1).

This paper is organized as follows. In Sec. II, our scheme is introduced after a brief review of the continuous QND measurement. Section III is devoted to the formalism of time evolution based on von Neumann's quantum measurement theory and embodied with the aid of the decomposition formula of an exponential operator. Numerical results are given in Sec. IV in two parameter regimes. The competition between unitary and nonunitary evolutions is also discussed there.

*Author to whom correspondence should be addressed. Electronic address: ogawa@cmpt01.phys.tohoku.ac.jp

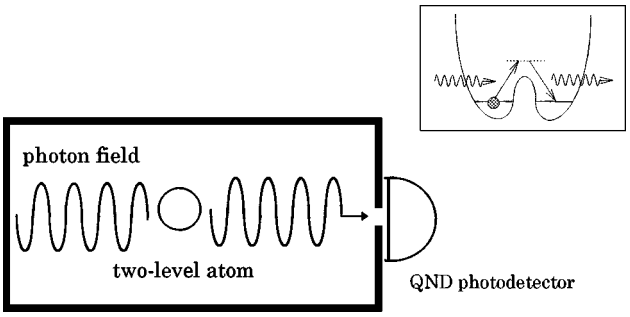

FIG. 1. Schematic illustration of our system. The cavity contains a two-level atom and a single-mode quantized photon field. The photon number inside the cavity is continuously measured by the QND photodetector at the right-hand side of the cavity. Inset: a physical model corresponding to the QND photodetector.

II. CONTINUOUS MEASUREMENT AND PRESENT SCHEME

In the context of the quantum measurement, temporal evolution of any measured quantity (signal) should be led from von Neumann's quantum measurement theory, regardless of the kind of measurement apparatus (probe). According to this principle, the quantum measurement process consists of two stages [4]. In the first stage, signal and probe become quantum-correlated through the interaction Hamiltonian $\hat{\mathcal{H}}_{\rm int}$, that is,

$$\hat{\rho}_{s-p}(t_0+t)=\hat{U}(t)\hat{\rho}_s(t_0)\otimes\hat{\rho}_p(t_0)\hat{U}^{\dagger}(t), \tag{1}$$

where $\hat{U}(t)=\exp(-i\hat{\mathcal{H}}_{\rm int}t/\hbar)$, $\hat{\rho}_s(t_0)$ $[\hat{\rho}_p(t_0)]$ are the initial density operator for the signal [probe], and $\hat{\rho}_{s-p}(t_0+t)$ is the total density operator at t_0+t. This process is reversible because the interaction is unitary. In the second stage, the probe is read out instantaneously, resulting in a new quantum state of the signal via nonunitary state reduction as

$$\hat{\rho}_s(t_0+t^+)=\frac{{\rm Tr}_p[\hat{\rho}_{s-p}(t_0+t)\otimes|X\rangle_{pp}\langle X|]}{{\rm Tr}_{s-p}[\hat{\rho}_{s-p}(t_0+t)\otimes|X\rangle_{pp}\langle X|]}, \tag{2}$$

where $\hat{\rho}_s(t_0+t^+)$ is the signal density operator just after the measurement and $|X\rangle_p$ is an eigenvector of the probe observable $\hat{X}_p$ with an eigenvalue X_p. Thus, the measurement process becomes irreversible only at the second stage.

The continuous photon counting [5,6] is not an exception to this principle, although the state reduction of the photon field occurs at every moment when the detector is active. In Ref. [7], the microscopic quantum theory of the continuous photodetection was proposed by one of the present authors based on von Neumann's theory and it was shown that the procedure correctly reproduces issues of the Srinivas-Davies model [5] for the photodetection.

One of the present authors considered the model that permits the photon number to be a QND observable, and provided a continuous QND (CQND) measurement scheme for the photon number [8]. The interaction Hamiltonian they proposed is

$$\hat{\mathcal{H}}_{\rm int}=\hbar g\hat{a}^{\dagger}\hat{a}(\hat{\sigma}_-+\hat{\sigma}_+), \tag{3}$$

where g is the coupling constant between the signal (photon field) and the probe (QND photodetector), $\hat{a}$ $(\hat{a}^{\dagger})$ is the photon annihilation (creation) operator, and $\hat{\sigma}_{\pm}$ is the flipping operator, which represents the transition from one state to the other in a degenerate bistable device. A good example here is a molecule with a double-quantum-well potential, as shown in the inset of Fig. 1. The state of a molecule initially prepared in the left valley can transit to the right through the virtual uppermost energy level with an infinitesimal lifetime, leading to a photoabsorption and a subsequent photoemission. If the state of the molecule initially prepared in the left valley is found in the right one after the interaction, a single photon has been detected; if the state of the atom is found to remain in the left valley, no photon has been detected. Thus, contrary to the photodetector made of a two-level atom [5–7], the QND photodetector can count a photon nondemolitionally.

Practically, the interaction Hamiltonian in Eq. (3) satisfies the QND conditions for the photon number $\hat{n}\equiv\hat{a}^{\dagger}\hat{a}$ [8,9]:

$$\begin{aligned}&\text{(a)}\ [\hat{\mathcal{H}}_{\rm photon},\ \hat{n}]=0,\\ &\text{(b)}\ [\hat{\mathcal{H}}_{\rm int},\ \hat{n}]=0,\\ &\text{(c)}\ [\hat{\mathcal{H}}_{\rm int},\ \hat{\sigma}_-]\neq 0,\\ &\text{(d)}\ \hat{\mathcal{H}}_{\rm int}\ \text{should be a function of}\ \hat{n},\end{aligned} \tag{4}$$

where $\hat{\mathcal{H}}_{\rm photon}=\hbar\omega(\hat{n}+\frac{1}{2})$. With the use of the procedure mentioned in Ref. [8], we describe (i) the one-count process at $t=t_0$ as

$$\hat{\rho}_s(t^+)\propto\hat{n}\hat{\rho}_s(t_0)\hat{n}, \tag{5}$$

and (ii) the no-count process during $t_0\leqslant t\leqslant t_0+\tau$ as

$$\hat{\rho}_s(t_0+\tau)\propto\exp\left(-\frac{\lambda}{2}\hat{n}^2\tau\right)\hat{\rho}_s(t_0)\exp\left(-\frac{\lambda}{2}\hat{n}^2\tau\right), \tag{6}$$

where $\lambda\equiv g^2\Delta t$. Here $\hat{\rho}_s(t^+)$ is the signal (photon field) density operator just after the one-count process, and τ is the time during which no photon is counted. The main idea of Ueda *et al.*'s theory lies in the introduction of a sequence of these two kinds of infinitesimal processes with an interaction time Δt, each of which represents a signal-probe coupling via unitary interaction followed by ''readout'' of the measuring probe.

The time evolution through the continuous measurement is nonunitary and its periodicity is broken via the time-irreversible state reduction of wave packets. Therefore, it is interesting to investigate whether a nonintegrable system bears quantum behaviors different from those of integrable systems and, in particular, whether the former shows temporal chaos.

Let us now employ the Jaynes-Cummings (JC) model without the rotating-wave approximation (RWA) (called the non-RWA JC model hereafter) and the QND photodetection as a quantum system and continuous measurement strategy.

The JC model has been recognized as the simplest and most effective model to treat the interaction between a two-

level atom and a single-mode quantized photon field [10]. In addition to its exact solvability within the RWA, the model provides a number of remarkable properties due to the quantum aspects of the field such as ''collapse and revival'' in the time domain [11]. The failure of the RWA, however, leads to somewhat different conclusions from those of the JC model with the RWA.

The non-RWA JC model is of interest in connection with ''quantum chaos.'' Its Hamiltonian is given by

$$\hat{\mathcal{H}}_{\text{system}}=\frac{1}{2}\hbar\omega_0\hat{S}_z+\hbar\omega\left(\hat{n}+\frac{1}{2}\right)+i\hbar\Omega\hat{S}_x(\hat{a}-\hat{a}^\dagger), \quad (7)$$

where $\hat{S}_z$ and $\hat{S}_x\equiv\hat{S}_-+\hat{S}_+$ are the Pauli spin matrices, and the constants ω_0, ω, and Ω are an energy separation of the two-level atom (with upper $|a\rangle$ and lower $|b\rangle$ levels), the frequency of the photon field, and a coupling constant between them (the vacuum Rabi frequency), respectively.

Our proposed scheme is illustrated in Fig. 1. A two-level atom and a single-mode quantized photon field are confined in a finite-Q cavity; they couple with each other through the interaction in Eq. (7). The cavity is supposed to have a small window, through which the continuous measurement, i.e., the QND photodetection is carried out. The leaked photons are continuously measured one by one by using the QND photodetector. Throughout the continuous measurement, the photon field keeps interacting with the two-level atom. In the next section, we shall develop the scheme for time evolution of the continuously measured quantum system.

Here we mention the reason for exploiting the QND photodetector (rather than the demolition-type photodetector in Ref. [5–7]) as the method of the continuous measurement. The average photon number will decrease toward zero if we employ the demolition-type photodetector regardless of initial photon states [6]. In other words, the photons in the cavity are still absorbed toward a vacuum state and the Bloch vector of the interacting two-level atom will cease to move sooner or later. Since we need to calculate the time evolution of the Bloch vector and compare the results with its classical counterpart, the QND-type photodetector should be used with which one can detect photons without a substantial decrease of the photon number relatively in the cavity.

III. MICROSCOPIC MODEL FOR TIME EVOLUTION

In our proposed scheme, the measured quantum system (the non-RWA JC model) is accompanied by two kinds of temporal evolutions. One is the *internal* evolution, which is time-reversible and described by the von Neumann equation of the density operator, $i\hbar d\hat{\rho}(t)/dt=[\hat{\mathcal{H}},\hat{\rho}(t)]$. The other is the time-irreversible *nonunitary* evolution due to the continuous measurement of the internal system. Since the latter process cannot be described by the orthodox von Neumann equation, we should apply von Neumann's quantum measurement theory to the evolution of our system, envisaging a combination of the unitary evolution and the subsequent instantaneous projection.

The total Hamiltonian of our system is given by a linear combination of the non-RWA JC model Hamiltonian in Eq. (7) and the interaction Hamiltonian in Eq. (3),

$$\hat{\mathcal{H}}_{\text{total}}=\hat{\mathcal{H}}_{\text{system}}+\hat{\mathcal{H}}_{\text{int}}. \quad (8)$$

Note that this total Hamiltonian no longer satisfies the QND measurement conditions for the photon number [9]. For each time interval, $[t_0,t_0+\Delta t]$, the initial state is expressed as

$$\hat{\rho}_{\text{total}}(t_0)=\hat{\rho}_{\text{system}}(t_0)\otimes|l\rangle\langle l|_{\text{detector}}. \quad (9)$$

Here $\hat{\rho}_{\text{system}}(t)$ is the density operator for the non-RWA JC model and $|l\rangle\langle l|_{\text{detector}}$ means that the QND photodetector is initially prepared in the ''left'' (l) valley.

First, the time evolution of the total density operator can be described as

$$\hat{\rho}(t_0+\Delta t)=\hat{U}(\Delta t)\hat{\rho}_{\text{total}}(t_0)\hat{U}^\dagger(\Delta t), \quad (10)$$

where

$$\hat{U}(\Delta t)\equiv\exp(-i\hat{\mathcal{H}}_{\text{total}}\Delta t/\hbar). \quad (11)$$

In this stage, the quantum correlation between the non-RWA JC model and the QND photodetector is established.

In the second stage, the density matrix Eq. (10) is adjusted according to the result of the readout information of the QND photodetector as

$$\hat{\rho}_{\text{system}}(t_0+\Delta t)=\frac{\text{Tr}_{\text{detector}}[\hat{\rho}(t_0+\Delta t)\otimes|r\rangle\langle r|_{\text{detector}}]}{\text{Tr}[\hat{\rho}(t_0+\Delta t)\otimes|r\rangle\langle r|_{\text{detector}}]}, \quad (12)$$

or

$$\hat{\rho}_{\text{system}}(t_0+\Delta t)=\frac{\text{Tr}_{\text{detector}}[\hat{\rho}(t_0+\Delta t)\otimes|l\rangle\langle l|_{\text{detector}}]}{\text{Tr}[\hat{\rho}(t_0+\Delta t)\otimes|l\rangle\langle l|_{\text{detector}}]}. \quad (13)$$

Equations (12) and (13) correspond to the one-count and no-count processes, respectively, and their probabilities are given in terms of the probability amplitudes $C(t)$'s as

$$P_{\text{one}}(t)=\sum_{n=0}^{\infty}[|C_{a,r,n}(t)|^2+|C_{b,r,n}(t)|^2], \quad (14)$$

$$P_{\text{no}}(t)=\sum_{n=0}^{\infty}[|C_{a,l,n}(t)|^2+|C_{b,l,n}(t)|^2], \quad (15)$$

respectively, where $P_{\text{one}}+P_{\text{no}}=1$.

Finally, the *new* QND photodetector, which is initially prepared in a prescribed state, is set to

$$\hat{\rho}_{\text{total}}(t_0+\Delta t)=\frac{\text{Tr}_{\text{detector}}[\hat{\rho}(t_0+\Delta t)\otimes|\ \rangle\langle\ |_{\text{detector}}]}{\text{Tr}[\hat{\rho}(t_0+\Delta t)\otimes|\ \rangle\langle\ |_{\text{detector}}]}\otimes|l\rangle\langle l|_{\text{detector}}, \quad (16)$$

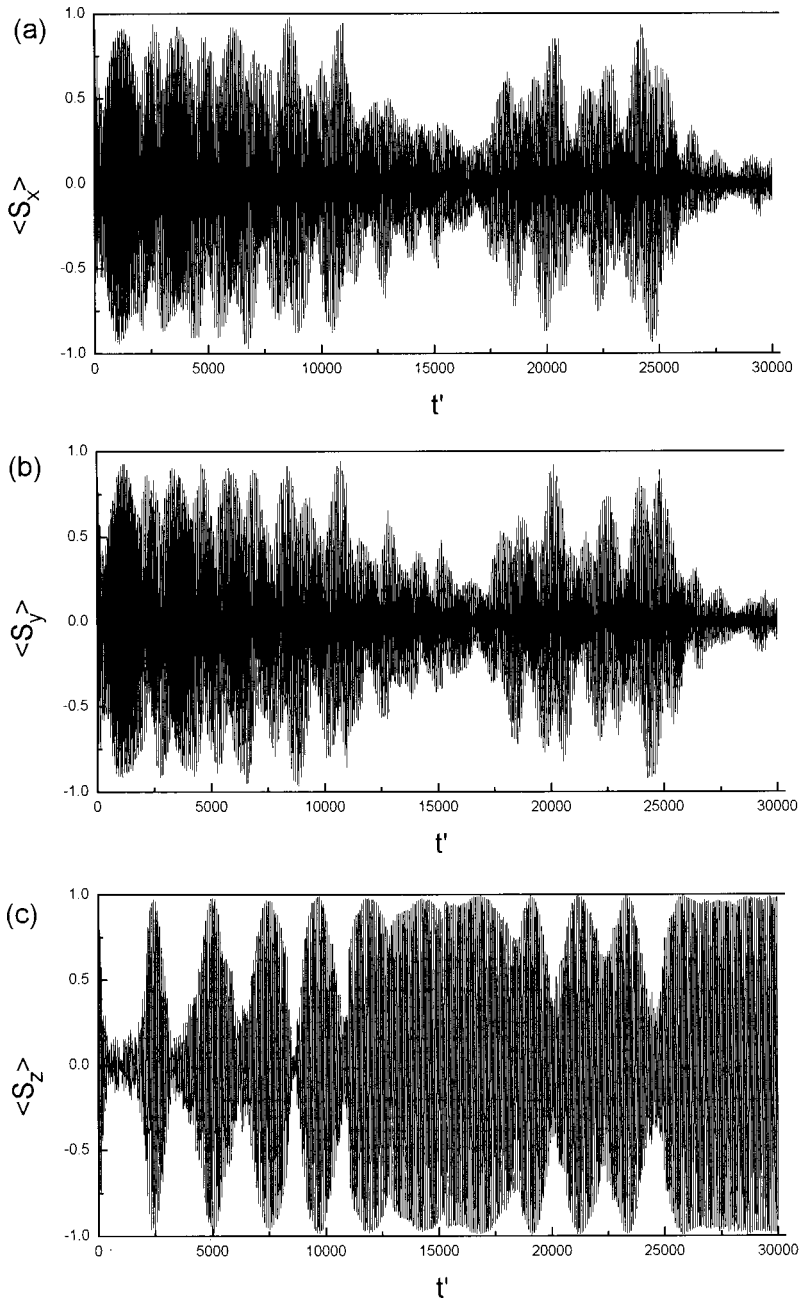

FIG. 2. Temporal evolution of the spin matrices calculated by the non-RWA JC model in WCR as a function of the normalized (dimensionless) time $t' \equiv t/\Delta t$: (a) $\langle \hat{S}_x \rangle$, (b) $\langle \hat{S}_y \rangle$, and (c) $\langle \hat{S}_z \rangle$. An initial state at $t'=0$ is $|a\rangle\langle a|$ (the upper level) for the atom part and $|\alpha\rangle\langle\alpha|$ (the coherent state) with $|\alpha|^2=15$ for the photon part. Numerical parameters are chosen as $\omega\Delta t=0.5$, $\Omega\Delta t=0.01$, and $g\Delta t=0.01$.

and the time evolution of the system is obtained by making successive operations from Eq. (9) through Eq. (16).

Now, a problem is to find an analytical expression for $\hat{U}(\Delta t)$ in Eq. (11), which is used in the practical calculations. Especially in the study of dynamical chaos, it is important to proceed with the calculations as precisely as possible to overcome the numerical errors due to computational calculations. Reflecting the classical nonintegrability underlying in the non-RWA JC model Hamiltonian in Eq. (7), the matrix elements of Eq. (11) cannot be written explicitly, contrary to the case of the RWA JC model.

We have recourse here to the second-order symmetric decomposition formula of an exponential operator, i.e., the Trotter formula [12],

$$e^{\hat{A}+\hat{B}} = e^{\hat{A}/2} e^{\hat{B}} e^{\hat{A}/2} [1 + o([\hat{A},\hat{B}])]. \tag{17}$$

This decomposition is valid for noncommutable operators $\hat{A}$ and $\hat{B}$ when explicit expressions for $\exp(\hat{A})$ and $\exp(\hat{B})$ could be given on the common bases. The advantage of Eq. (17) is that, when applied to the density operator, it keeps precisely both the unitary and symplectic nature of the quantum dynamics. In our case, we decompose the development operator Eq. (11) into two integrable components as

$$\exp\left[-\frac{i}{\hbar}(\hat{\mathcal{H}}_1 + \hat{\mathcal{H}}_2)\Delta t \right] \simeq \exp\left(-\frac{i}{2\hbar}\hat{\mathcal{H}}_1 \Delta t \right) \exp\left(-\frac{i}{\hbar}\hat{\mathcal{H}}_2 \Delta t \right) \exp\left(-\frac{i}{2\hbar}\hat{\mathcal{H}}_1 \Delta t \right), \tag{18}$$

where

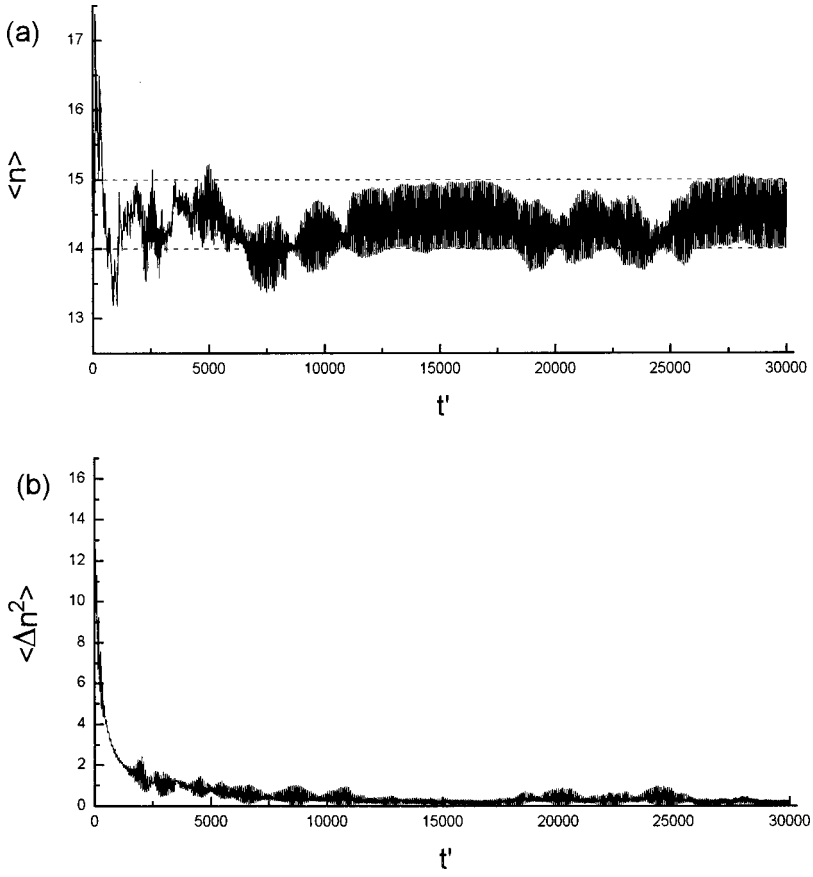

FIG. 3. Temporal evolution calculated by the non-RWA JC model in WCR as a function of the normalized time $t' \equiv t/\Delta t$: (a) the mean photon number $\langle \hat{n} \rangle$ and (b) the photon number variance $\langle \Delta \hat{n}^2 \rangle$. As the measurement proceeds, the mean photon number oscillates between certain adjacent integers stochastically. Numerical parameters are the same as in Fig. 2.

$$\hat{\mathcal{H}}_1 = \frac{1}{2}\hbar\omega_0 \hat{S}_z + \hbar\omega\left(\hat{n} + \frac{1}{2}\right) + i\hbar\Omega(\hat{S}_+ \hat{a} - \hat{a}^\dagger \hat{S}_-) + \hbar g \hat{n}(\hat{\sigma}_- + \hat{\sigma}_+), \tag{19}$$

$$\hat{\mathcal{H}}_2 = i\hbar\Omega(\hat{S}_- \hat{a} - \hat{a}^\dagger \hat{S}_+). \tag{20}$$

It should be noted that the time evolution of our model consists in principle of a sequence of the infinitesimal processes. While we need to calculate the unitary evolution for each short-time duration $[t_0,\ t_0 + \Delta t]$, the above approximation is quite suitable for our study.

IV. RESULTS OF CALCULATIONS

In this section, we calculate several quantities of the two subsystems (a two-level atom and a quantized photon field) with the use of the scheme in the preceding section. Their temporal evolution is derived by the multiplication of matrices consisting of the density matrix and the unitary matrix, and by the subsequent reduction of the matrix elements corresponding to the readout information, where the counting pulses are produced by a random noise generator depending on the probability of the one-count or no-count processes in Eqs. (14) and (15).

We perform numerical calculations in two cases of the ratio between ω $(\approx \omega_0)$ and Ω, i.e., (i) $\omega/\Omega \gg 1$ and (ii) $\omega/\Omega = \mathcal{O}(1)$. In Sec. IV A, the results in the case (i) are presented, and Sec. IV B is devoted to the case (ii). The cases (i) and (ii) will hereafter be called a ''weak-coupling regime (WCR)'' and a ''strong-coupling regime (SCR),'' respectively. The SCR can be realized when a collection of many identical atoms are confined to a region small compared with the wavelength of the photon field with high density [13,14]. In this paper, we shall concentrate only on the resonance case $\omega_0 = \omega$.

A. Results in the WCR

In general, the ratio between ω and Ω controls the range of the validity of the RWA. In the WCR $(\omega/\Omega \gg 1)$, which is the condition satisfied in conventional cavity QED experiments [15], the contribution of the counter-rotating terms, $\hbar\Omega\hat{S}_-\hat{a}$ and $\hbar\Omega\hat{a}^\dagger\hat{S}_+$, are averaged out on a time scale of $1/\omega$ [11]. Therefore, the RWA is a good approximation in the WCR.

Figures 2(a), 2(b), and 2(c) show the temporal evolution of the spin matrices, $\langle \hat{S}_x \rangle$, $\langle \hat{S}_y \rangle$, and $\langle \hat{S}_z \rangle$, in the WCR, respectively. Note that $\langle \hat{S}_z \rangle$ corresponds to the atomic inversion, that is, the population difference between upper and lower levels. The initial density operator at $t = 0$ is assumed to be a coherent state $\hat{\rho}_{\text{photon}}(0) = |\alpha\rangle\langle\alpha|$ with $n_0 \equiv |\alpha|^2 = 15$ for the field part multiplied by an upper state $\hat{\rho}_{\text{atom}}(0) = |a\rangle\langle a|$ for the atom part. Collapses and revivals of the Rabi oscillation are found in the temporal evolution of the population inversion [see Fig. 2(c)], which is a typical feature of the RWA JC model with the initially coherent state for the photon part [11]. Unlike the case in which the continuous QND measurement has not been done, however, the Rabi oscillation revives almost *completely*: $\langle \hat{S}_z \rangle$ oscillates from -1 to 1.

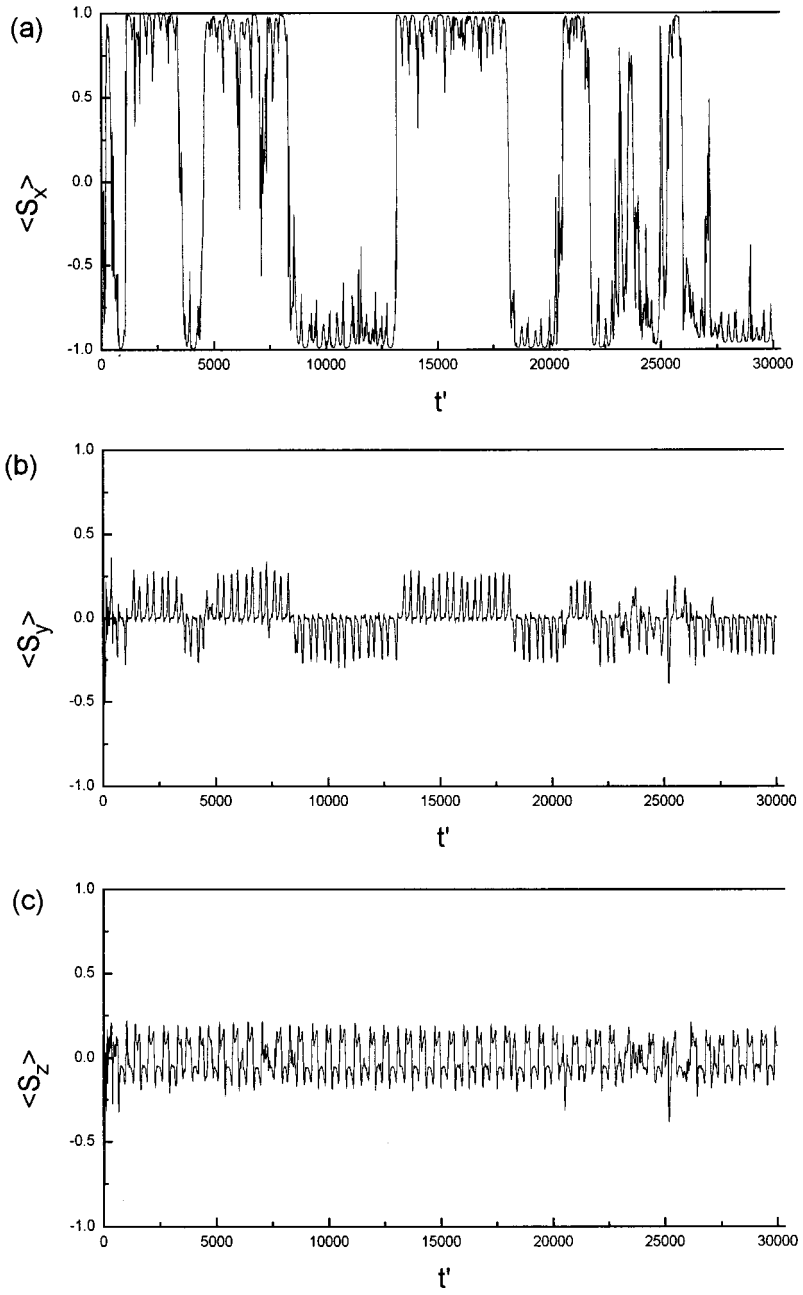

FIG. 4. Temporal evolution of the spin matrices calculated by the non-RWA JC model in SCR as a function of the normalized time $t' \equiv t/\Delta t$: (a) $\langle \hat{S}_x \rangle$, (b) $\langle \hat{S}_y \rangle$, and (c) $\langle \hat{S}_z \rangle$. An initial state at $t' = 0$ is chosen to be the same as in Fig. 2. Numerical parameters are chosen as $\omega \Delta t = 0.01$, $\Omega \Delta t = 0.01$, and $g \Delta t = 0.01$.

The above curious result can be understood with the use of the temporal evolution of the mean photon number $\langle \hat{n} \rangle$ and the photon-number variance $\langle \Delta \hat{n}^2 \rangle \equiv \langle \hat{n}^2 \rangle - \langle \hat{n} \rangle^2$ in Figs. 3(a) and 3(b). As mentioned in Ref. [11], the revival phenomenon is attributed to the fluctuation of the quantum Rabi frequency, proportional to the photon number. The initial coherent state has the fluctuation of the photon number, which is equal to the mean photon number, and this has been suppressed through the temporal evolution via the CQND measurement. The mean photon number is initially staggered by the measurement back action of the QND photodetection, as plotted in Fig. 3(a), but it gradually converges, accompanied by the small oscillation as the measurement proceeds. One can understand the dynamics more clearly in Fig. 3(b), where the photon number variance shows an oscillatory decay. The Rabi oscillation is the signature of the unitary evolution of the JC model, whereas the decay is caused by the CQND measurement of the photon number (i.e., nonunitary evolution). Thus, in the WCR, the characteristic behavior of both unitary and nonunitary evolutions appears in the temporal evolution.

Although the time series of Figs. 2(a), 2(b), and 2(c) are very complicated, we cannot expect quantum chaos in this WCR, where the RWA is a good approximation. Actually, if the counter-rotating terms in Eq. (7) could be neglected, the corresponding classical nonintegrable system is reduced to the integrable system. So the system never yields temporal chaos but does yield (quasi)periodic motion only.

Here we mention the dependence of the temporal evolution on g, which determines the measurement strength. In the WCR, the photon state is reduced to a photon number state as the measurement proceeds, regardless of the initial states. The ratio between g and ω or Ω merely alters the time scale of the convergence towards the photon number state. We

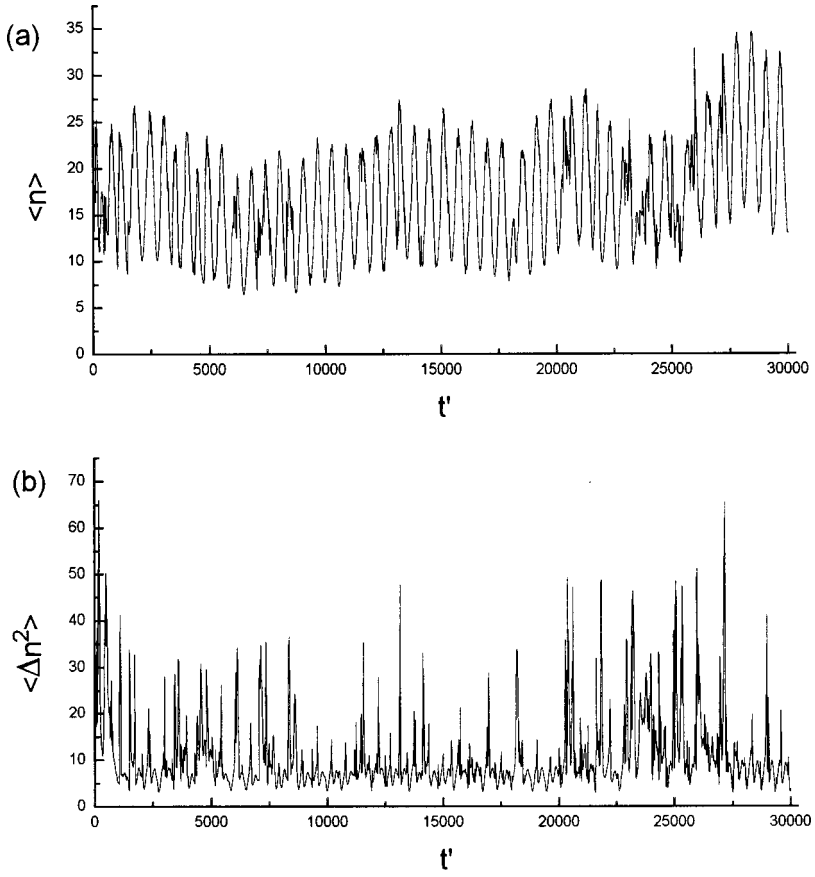

FIG. 5. Temporal evolution calculated by the non-RWA JC model in SCR as a function of the normalized time $t' \equiv t/\Delta t$: (a) the mean photon number $\langle \hat{n} \rangle$ and (b) the photon number variance $\langle \Delta \hat{n}^2 \rangle$. Numerical parameters are the same as in Fig. 4.

shall therefore not pay attention to the ratio. If g is much larger than ω and Ω, does the Rabi oscillation cease by the strong measurement to the system? The answer is ''no.'' The Rabi oscillation never stops even if g is infinitely large. Disappearance of the Rabi oscillation means that the atomic inversion and the photon field are trapped in a certain level (upper or lower state) and a certain photon number state, respectively. In other words, the total system provides the QND measurements for the atomic inversion and the photon number. The total Hamiltonian in Eq. (8), however, satisfies the QND conditions [9] for neither the inversion $\hat{S}_z$ nor the photon number $\hat{n}$. Therefore, the photon number variance shown in Fig. 3(b) never converges to zero although it decays, and the Rabi oscillation remains forever even if g is infinitely large.

B. Results in the SCR

In the SCR, as predicted by Tavis and Cummings [16], the RWA fails and we can expect chaotic behavior in the temporal evolution. Figures 4(a), 4(b), and 4(c) show the time evolution of the spin matrices, $\langle \hat{S}_x \rangle$, $\langle \hat{S}_y \rangle$, and $\langle \hat{S}_z \rangle$, in the SCR. The initial density matrix is chosen to be the same as in the WCR. Comparing Fig. 4(c) with Fig. 2(c), one finds that the revival phenomenon of the population inversion does not appear in contrast to the WCR.

The corresponding time evolutions of the mean photon number and the photon number variance are given in Figs. 5(a) and 5(b), respectively. A drastic difference from the results in the WCR can be seen from these figures, that is, the mean photon number never settles down as in Fig. 3(a), even when we enforce the CQND measurement on the photon number. Figure 5(b) shows that the photon number variance does not decay through the time evolution but shows intermittent pulsation, despite the fact that we use the continuous readout information to estimate the photon number in the cavity.

Generally in an interacting system consisting of a two-level atom and a quantized photon field under the RWA, the state of the atom can change from the upper-level to the lower-level (from lower to upper) state via one-photon emission (absorption). It indicates that the Hilbert space initially prepared is *closed* as the series of (2×2) matrices throughout the time development, and it does not spread further. Then, the photon number variance does not increase over the long time, but remains relatively constant involving small oscillations, whereas the non-RWA JC model in Eq. (7) permits the atomic state to change from the upper-level to the lower-level state via one-photon emission *or* absorption, and vice versa. It leads to the *diffusion in the Hilbert space*, corresponding to the increase of the photon-number variance in the time evolution. On the contrary, the CQND measurement of the photon number has the tendency to suppress the photon-number variance with the use of the readout information of the photon number. In the SCR, where the RWA is not a good approximation and the counter-rotating terms work more effectively than in the WCR, the competition between these opposite mechanisms occurs, leading to the remarkable and unpredictable time series.

Figure 6 shows the power spectrum of $\langle \hat{S}_x \rangle$,

$$P(\omega) \equiv \left| \frac{2}{t_{\max}} \int_0^{t_{\max}} \langle \hat{S}_x \rangle e^{-i\omega t} dt \right|, \tag{21}$$

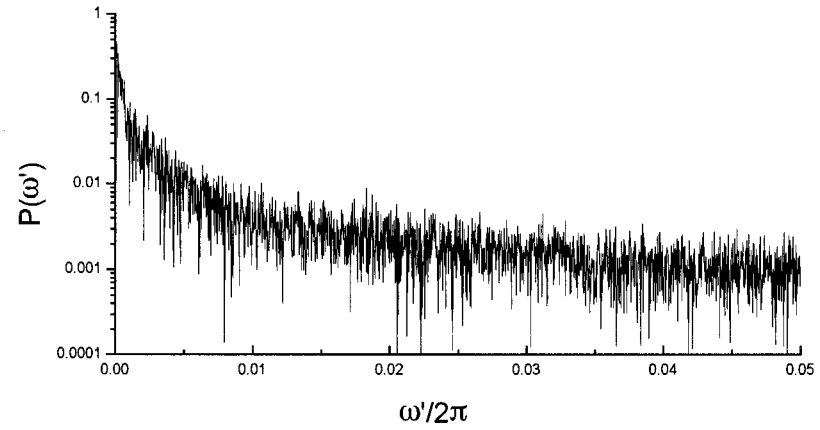

FIG. 6. Power spectrum of $\langle \hat{S}_x \rangle$ calculated by the non-RWA JC model in SCR as a function of the normalized (dimensionless) frequency $\omega'/2\pi \equiv \Delta t/t$. The spectrum corresponds to the temporal evolution in Fig. 4(a).

corresponding to Fig. 4(a). This quantity is often employed as the diagnostics of quantum chaos. In a spin-boson interacting system such as the non-RWA JC model, the dynamical symmetry in spin matrices is broken and the interaction component $\langle \hat{S}_x \rangle$ shows a curious behavior, as conjectured from the Hamiltonian in Eq. (7). In addition, the time evolution of $\langle \hat{S}_x \rangle$ is strongly disturbed via the continuous measurement of the photon field. We note that the remaining components, $\langle \hat{S}_y \rangle$ and $\langle \hat{S}_z \rangle$, show qualitatively similar properties. Then we shall confine ourselves to the discussion about temporal chaos with respect to $\langle \hat{S}_x \rangle$. One can find a broadband and a continuous component in Fig. 6, indicating the temporal chaos.

For comparison, we calculated power spectra of the corresponding classical model and the non-RWA JC model *without* the CQND measurement ($g=0$) in Figs. 7(a) and 7(b), respectively. The classical equations of motion are obtained via decorrelation of the atomic and photon operators when the Heisenberg equations are averaged for observables, leading to the Maxwell-Bloch equations [13]. In the classical counterpart, one finds a broadband, continuous component in its spectrum, which indicates that the temporal evolution is chaotic without any signature of stable periodic evolution. Actually, the temporal evolution shows genuine chaos, characterized by standard diagnostics of positive Lyapunov exponents [13,14]. In the quantum version of the model *without* the CQND measurement, however, chaos is excluded due to the linearity of the Schrödinger equation. The spectrum is not continuous but accompanied by discrete line spectra, which indicates that the temporal evolution is quasiperiodic rather than chaotic. Thus we conclude that the chaotic prop-

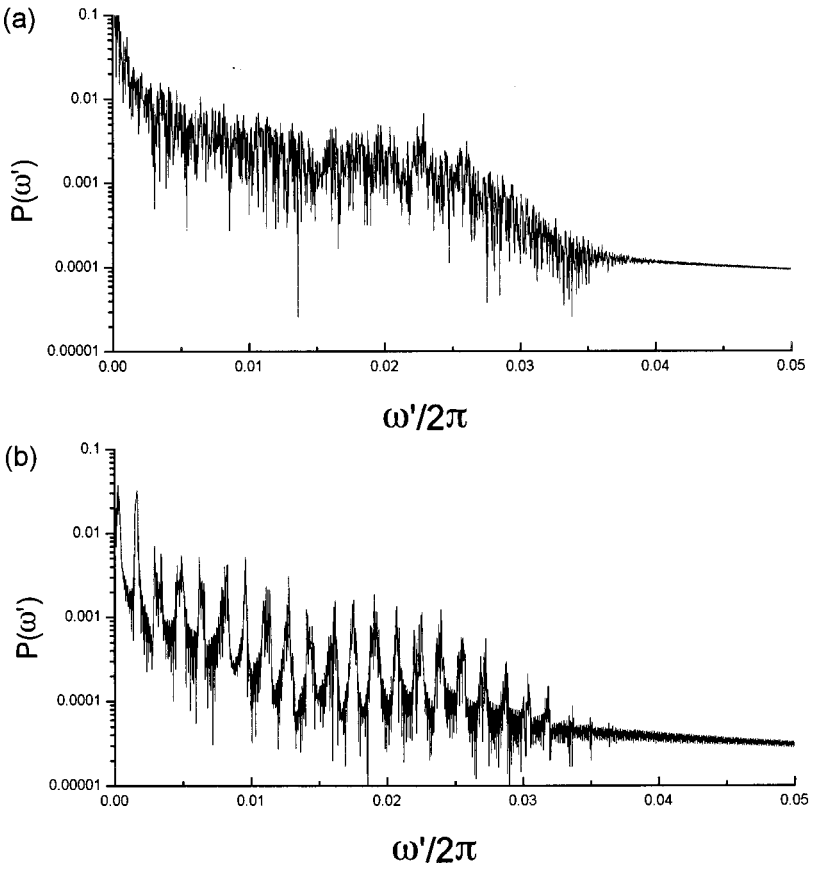

FIG. 7. Power spectrum of $\langle \hat{S}_x \rangle$ calculated by (a) the *classical* Maxwell-Bloch equations and (b) the *unmeasured* non-RWA JC model in SCR as a function of the normalized (dimensionless) frequency $\omega'/2\pi \equiv \Delta t/t$. Numerical parameters are the same as in Fig. 4 except for the measurement strength $g=0$. Compare with Fig. 6.

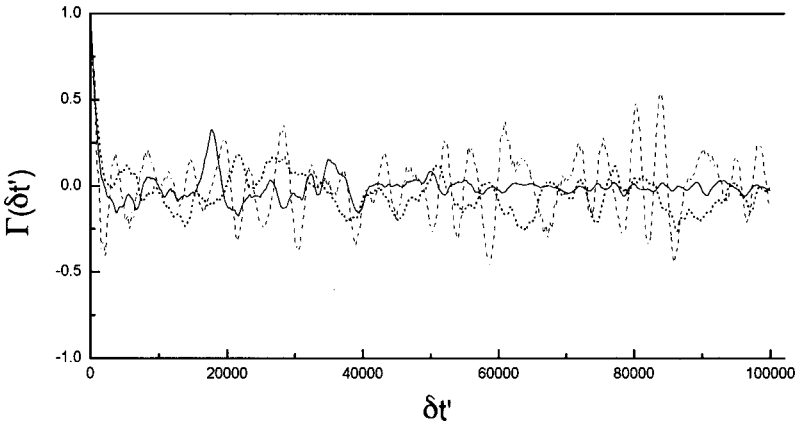

FIG. 8. Autocorrelation function of $\langle \hat{S}_x \rangle$ for the CQND-measured non-RWA JC model (solid line), the unmeasured non-RWA JC model (dashed line), and the classical Maxwell-Bloch equations (dotted line) as a function of the normalized (dimensionless) time difference $\delta t' \equiv \delta t/\Delta t$. Numerical parameters are the same as in Fig. 4.

erties inherent in the non-RWA JC model, usually suppressed by the linearity of the Schrödinger equation, are recovered due to the breakdown of time reversibility under the CQND measurement.

To quantify this chaotic signature, autocorrelation functions

$$\Gamma(\delta t) \equiv \frac{\langle S_x(t) S_x(t+\delta t) \rangle_t - \langle S_x(t) \rangle_t^2}{\langle S_x^2(t) \rangle_t - \langle S_x(t) \rangle_t^2} \tag{22}$$

are plotted in Fig. 8. Here $\langle\ \rangle_t$ means the average over the time, $\lim_{T\to\infty}(1/T)\int_0^T \cdots dt$. Contrary to the oscillatory correlation, which retains a long time for the *unmeasured* quantum model, we see the decaying correlation functions followed by noisy ripples for both the classical and the continuously measured quantum versions, indicating the lack of quantum recurrence.

For classical systems there is no controversy about how to define chaotic behavior; classical chaos means very sensitive dependence on an initial condition of trajectories, and its properties can be checked by comparing the maximal Lyapunov exponent. In the case of quantum chaos, on the other hand, there is no such hard number that measures the rate of exponential separation of neighboring trajectories, because the concept of the ''neighboring trajectories'' cannot be well defined in the quantum theory due to the uncertainty principle. So we can refer to this chaotic behavior as ''weak chaos,'' characterized by both the broad continuous power spectrum and the decaying correlation function.

Last, we mention the dependence of the *continuous* measurement on the duration Δt during which the interaction is switched on between the system and the QND photodetector. To neglect the possibility of more than one photon being detected in each duration, one has to take the limit $\Delta t \to 0$ [7,8]. In addition, to justify the decomposition formula of an exponential operator in Eq. (18), one must set Δt less than $1/\omega$, $1/\Omega$, and $1/g$. However, if Δt is equal to zero, the quantum correlation is not established in Eq. (10) so that the information of the system is not copied onto the QND photodetector. Thus, Δt should be small (but nonzero) enough to satisfy $\omega \Delta t \ll 1$, $\Omega \Delta t \ll 1$, and $g \Delta t \ll 1$.

V. SUMMARY

The time evolution of a continuously measured (classically nonintegrable) quantum system, i.e., the non-RWA JC model under the continuous QND photodetection, is investigated as one of the candidates that has the possibility of showing temporal chaos within a quantum theory. We have developed the microscopic theory of time evolution based on von Neumann's quantum measurement theory and had recourse to the decomposition formula of an exponential operator. The unitary process originating from an internal time evolution and the nonunitary process due to the continuous QND measurement compete with each other in the time domain. Especially in the strong-coupling regime, the quantum system shows chaotic time evolution, characterized by both the broad continuous power spectrum and the decaying correlation function. In our system, the latent chaotic properties of the non-RWA JC model, suppressed by the linearity in the time-dependent Schrödinger equation, clearly emerge owing to the breakdown of the time reversibility in the CQND measurement process. We then expect that *nonintegrable quantum systems can yield ''weak chaos'' due to the breakdown of unitarity* in the course of their temporal evolution.

Last we note that in the CQND measurement process, results of a measurement are provided in an *indeterministic* way. One cannot predict the observed value in advance. Therefore the quantum chaos in the CQND measurement inevitably involves stochasticity. The situation in which the QND photodetector is switched on but the readout information in discarded (called the nonreferring measurement process) [6,8] is left for a future study.

ACKNOWLEDGMENTS

The authors would like to thank N. Imoto at NTT Basic Research Laboratories for valuable comments and fruitful discussions. T.F. is grateful to Y. Takane, S. Kawabata, and T. Maki for continuous encouragement, and K.N. thanks M. Berry for a critical comment on the decoherence. This work is supported by a Grant-in-Aid for Scientific Research on Priority Areas, ''Mutual Quantum Manipulation of Radiation Field and Matter,'' from the Ministry of Education, Science, Sports and Culture of Japan.

[1] See, e.g., *Chaos and Quantum Physics*, Proceedings of the Les Houches Summer School, Course LII, edited by M. J. Giannoni, A. Voros, and J. Zinn-Justin (North-Holland, Amsterdam, 1991).
[2] W. H. Zurek and J. P. Paz, Phys. Rev. Lett. **72**, 2508 (1994).
[3] Emergence of chaos in quantum systems via nonunitary evolution is discussed in K. Nakamura, *Quantum Versus Chaos* (Kluwer Academic, Dordrecht, 1997).
[4] J. von Neumann, *Mathematical Foundations of Quantum Mechanics* (Princeton University Press, Princeton, 1955).
[5] M. D. Srinivas and E. B. Davies, Opt. Acta **28**, 981 (1981); **29**, 235 (1982).
[6] M. Ueda, N. Imoto, and T. Ogawa, Phys. Rev. A **41**, 3891 (1990).
[7] N. Imoto, M. Ueda, and T. Ogawa, Phys. Rev. A **41**, 4127 (1990).
[8] M. Ueda, N. Imoto, H. Nagaoka, and T. Ogawa, Phys. Rev. A **46**, 2859 (1992).
[9] N. Imoto, H. A. Haus, and Y. Yamamoto, Phys. Rev. A **32**, 2287 (1985), and references therein.
[10] E. T. Jaynes and F. W. Cummings, Proc. IEEE **51**, 89 (1963); B. W. Shore and P. L. Knight, J. Mod. Opt. **40**, 1195 (1993).
[11] See, e.g., P. Meystre and M. Sargent III, *Elements of Quantum Optics* (Springer-Verlag, Berlin, 1991); D. F. Walls and G. J. Milburn, *Quantum Optics* (Springer-Verlag, Berlin, 1994).
[12] H. F. Trotter, Proc. Am. Math. Soc. **10**, 545 (1959); M. Suzuki, J. Stat. Phys. **43**, 883 (1986); J. Phys. Soc. Jpn. **61**, 3015 (1992).
[13] P. W. Milonni, J. R. Ackerhalt, and H. W. Galbraith, Phys. Rev. Lett. **50**, 966 (1983); R. F. Fox and J. Eidson, Phys. Rev. A **34**, 482 (1986); J. Eidson and R. F. Fox, *ibid.* **34**, 3288 (1986).
[14] P. W. Milonni, M.-L. Shih, and J. R. Ackerhalt, *Chaos in Laser-Matter Interactions* (World Scientific, Singapore, 1987).
[15] See, e.g., P. R. Berman, *Cavity Quantum Electrodynamics* (Academic Press, Boston, 1994), and references therein.
[16] M. Tavis and F. W. Cummings, Phys. Rev. **170**, 379 (1968); **188**, 692 (1969).